

## The Electrooxidation of Methanol in the Potential Region of Platinum–Oxygen Layer

Hiroshi MATSUI\* and Akira KUNUGI

Department of Chemical Science and Technology, Faculty of Engineering, The University of Tokushima, Minamijosanjima-cho, Tokushima 770

(Received October 14, 1989)

Methanol oxidation at a platinum electrode in 0.5 mol dm<sup>-3</sup> sulfuric acid at high potentials was retarded by the formation of both an oxygen layer and a new type of retarding substance from methanol. The presence of the retarding substance was confirmed by the oxygen-deposition method. During retardation due to the formation of an oxygen layer, the rate of methanol oxidation both decreased and increased with increasing oxygen coverage and potential, respectively. The reverse effects of oxygen coverage and potential concurrently occurred when the potential was a variable. At low oxygen coverage, the decreased effect of oxygen coverage was more remarkable than the increased effect of the potential, while the order of the remarkableness was reversed at middle coverage. The reversal of the order could be explained in terms of a catalytic reduction of the oxygen layer with methanol.

It is well-known<sup>1–3)</sup> that the oxidation of methanol at a platinum electrode in acid solutions is remarkably retarded in the presence of the platinum–oxygen layer. A similar retardation has also been observed in the oxidation of ethanol,<sup>4–6)</sup> formaldehyde,<sup>1,7)</sup> formic acid,<sup>1,8)</sup> etc.<sup>1)</sup>

The retardation of these oxidations is considerably complex. That is, the oxidation rate remarkably decreases with increasing oxygen coverage at low coverage, while at middle coverages it increases. Both the decrease and increase in the oxidation rate are explained in terms of a blocking of the reaction sites due to the oxygen species and a change in the chemical kind of oxygen species, e.g., PtOH→PtO.<sup>1,6)</sup> However, no quantitative verification has been given for the relationship between the oxidation rate and the coverage with a particular oxygen species.

The retardation of methanol oxidation at very small oxygen coverage also seems to be too remarkable to be explained in terms of the formation of an oxygen layer. Recently, methanol oxidation in the absence of an oxygen layer was found to be retarded by the accumulation of formaldehyde in the vicinity of the electrode surface.<sup>9)</sup> This retardation can also occur in the presence of the oxygen layer.

The aim of the present paper is to examine the kinetics of retardation due to the formation of the oxygen layer, and to confirm the presence of another type of retardation. The net retardation due to the formation of an oxygen layer was explained in terms of a single rate equation, and the extraordinary rate of the methanol oxidation at 0.8–0.9 V was due to the formation of new retarding adsorbates from methanol.

### Experimental

In order to minimize the effects of solution impurities on the reaction rate, a roughened platinum electrode with a roughness factor of 23 was used. The cell, reagents, and the procedures for measuring the rate of the methanol oxidation

at a constant potential were the same as those described in a previous paper.<sup>9)</sup>

The oxygen coverages,  $\theta_{\text{PtO}}$ , were expressed by

$$\theta_{\text{PtO}} = Q_{\text{PtO}}/2Q_{\text{H}}^0, \quad (1)$$

where  $Q_{\text{H}}^0$  is the charge required to fully cover the electrode surface in the absence of methanol, and  $\theta_{\text{PtO}}$  is that required to reduce the oxygen layer. The values of  $Q_{\text{H}}^0$  and  $\theta_{\text{PtO}}$  were determined by using the potential sequence shown in Fig. 1A.

***i*-*E* Curves:** The effect of preoxidation on the rate of

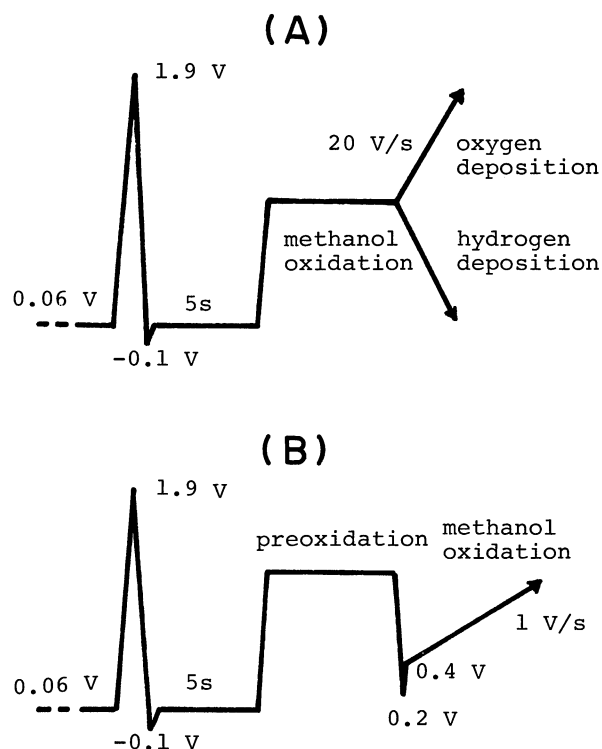


Fig. 1. Potential sequence for measuring coverage and *i*-*E* curves.

methanol oxidation was examined after a reduction of the oxygen layer by using the potential sequence shown in Fig. 1A. The presence of retarding adsorbates from methanol was confirmed by the oxygen-deposition method shown in Fig. 1B.

All of the experiments were carried out at 0°C and a methanol concentration of 0.1 mol dm<sup>-3</sup>. This concentration is convenient for a kinetic investigation of the methanol oxidation, because almost all of the products are carbon dioxide. All of the potentials were referred to a reversible hydrogen electrode (RHE) in 0.5 mol dm<sup>-3</sup> H<sub>2</sub>SO<sub>4</sub>.

## Results and Discussion

**Rate of Methanol Oxidation in the Presence of Oxygen Layer.** In the presence of an oxygen layer, the net rate,  $i_M$ , of the methanol oxidation can be expressed by

$$i_M = i_t - i_{\text{PtO}}^F, \quad (2)$$

where  $i_t$  and  $i_{\text{PtO}}^F$  are the overall rate and the rate of oxygen-layer formation, respectively. The  $i_{\text{PtO}}^F$  in the presence of methanol could be approximated by that in its absence, for the following results: (1) The  $\theta_{\text{PtO}}$  is slightly influenced by the presence of methanol, as can be seen from Fig. 2. (2) The  $i_{\text{PtO}}^F$  values were much smaller than  $i_t$  after about 0.5 s from the start of oxidation, as can be seen from Fig. 3. Thereafter,  $i_M$  was determined according to Eq. 2.

**Retardation of Methanol Oxidation.** Figure 4 shows the potentiostatic  $i_M$ - $E$  curves for the oxidation of methanol at an oxidation time of 10 s. Log  $i_M$  linearly increased with increasing potential up to about 0.75 V; at higher potentials it remarkably deviated from a linear line toward the downward direction, i.e., the methanol oxidation was remarkably retarded. The log  $i_M$ - $E$  curve had a minimum at about 1.15 V, suggesting that the retardation mechanism is

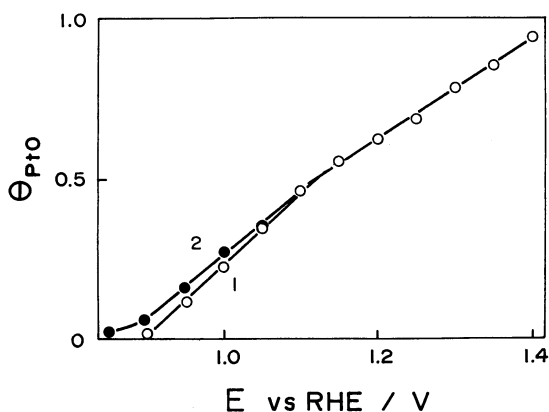


Fig. 2. Variation in oxygen coverage with potential, oxidation time 10 s. Solutions: (1) 0.1 mol dm<sup>-3</sup> CH<sub>3</sub>OH+0.5 mol dm<sup>-3</sup> H<sub>2</sub>SO<sub>4</sub>; (2) 0.5 mol dm<sup>-3</sup> H<sub>2</sub>SO<sub>4</sub>.

complex.

Figure 5 shows the variation in  $i_M$  with  $\theta_{\text{PtO}}$  at several potentials. A linear relationship between log

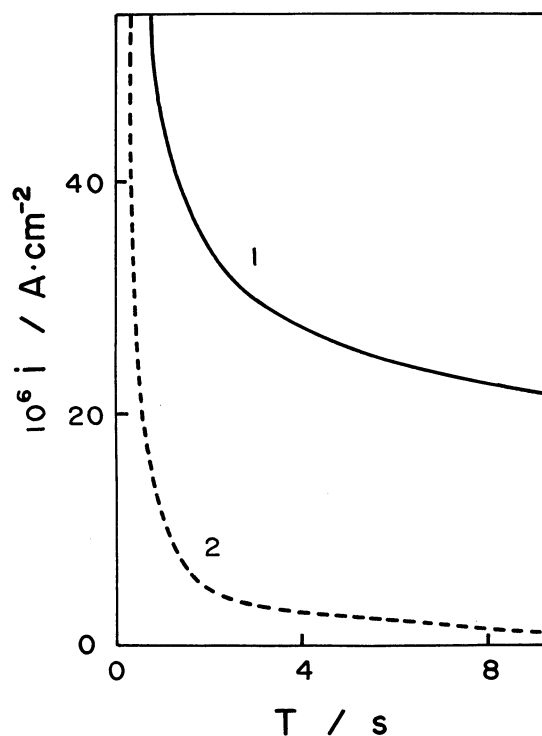


Fig. 3. Variation in oxidation rate at 1.3 V with time. Solutions: (1) 0.1 mol dm<sup>-3</sup> CH<sub>3</sub>OH+0.5 mol dm<sup>-3</sup> H<sub>2</sub>SO<sub>4</sub>; (2) 0.5 mol dm<sup>-3</sup> H<sub>2</sub>SO<sub>4</sub>.

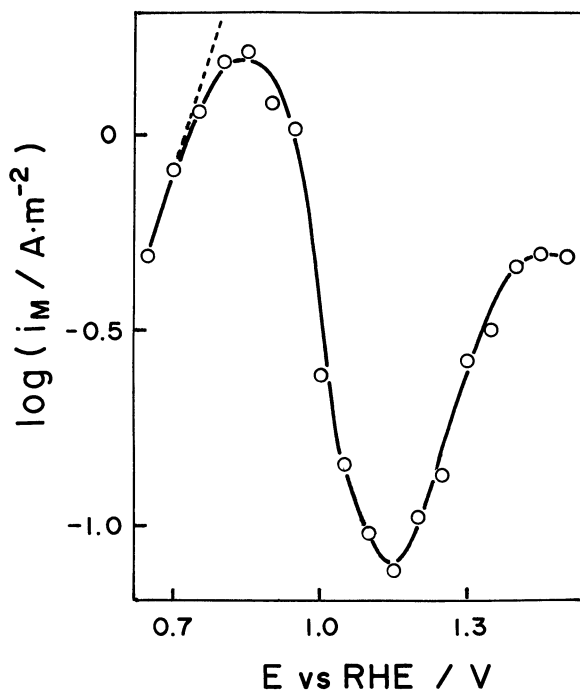


Fig. 4. Variation in oxidation rate with potential. 0.1 mol dm<sup>-3</sup> CH<sub>3</sub>OH+0.5 mol dm<sup>-3</sup> H<sub>2</sub>SO<sub>4</sub>. Oxidation time 10 s.

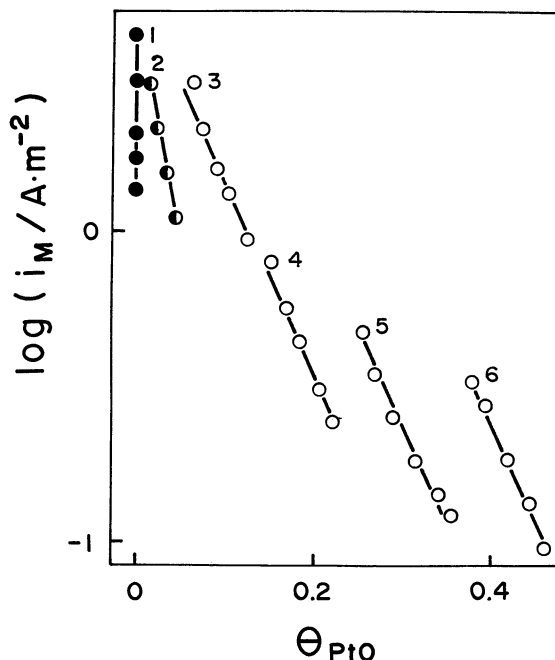


Fig. 5. Variation in oxidation rate with oxygen coverage  $0.1 \text{ mol dm}^{-3} \text{ CH}_3\text{OH} + 0.5 \text{ mol dm}^{-3} \text{ H}_2\text{SO}_4$ . Potentials (V): (1) 0.80; (2) 0.90; (3) 0.95; (4) 1.00; (5) 1.05; (6) 1.10.

$i_M$  and  $\theta_{\text{PtO}}$  was valid at each potential of 0.8–1.5 V. The slopes of the linear lines were  $-6.74$  over the entire potential range of 0.95–1.10 V, while in the range 0.8–0.9 V the slope decreased with decreasing potential. The cause of the retardation in each potential range of 0.8–0.9 and 1.0–1.5 V differed from each other, as described in the following sections. Therefore, we separately discuss the retardations of the methanol oxidation in these potential ranges.

**A) Retardation at 1.0–1.5 V:** The linear lines in this potential range of Fig. 5 can be expressed by

$$\log i_M = a_1 - 6.74 \theta_{\text{PtO}}, \quad (3)$$

where  $a_1$  is a constant depending on the potential. The  $a_1$  values were determined by extrapolating the linear line to  $\theta_{\text{PtO}}=0$ . As can be seen from Fig. 6, two linear relationships were valid between  $a_1$  and the potential in the potential range of about 1.0–1.25 and 1.25–1.4 V, respectively. Both relationships were expressed by

$$a_1 = a_2 + b_2 \cdot E, \quad (4)$$

where  $a_2$  and  $b_2$  are constants which depend on the potential range. Moreover, two linear relationships were valid between  $\theta_{\text{PtO}}$  and the potential in the potential ranges of about 0.9–1.15 and 1.2–1.5 V, respectively, as can be seen from Fig. 2. These relationships are also given by

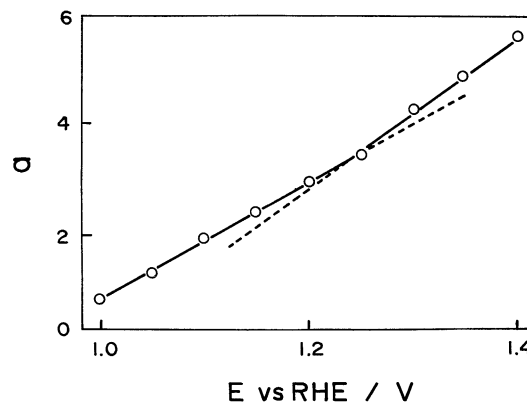


Fig. 6. Variation in  $a_1$  with potential,  $0.1 \text{ mol dm}^{-3} \text{ CH}_3\text{OH} + 0.5 \text{ mol dm}^{-3} \text{ H}_2\text{SO}_4$ , oxidation time 10 s.

Table 1. Parameters in Kinetic Equations for Formation of Oxygen Layer and Methanol Oxidation

$\log i_M = a_2 + b_2 \cdot E - 6.74 \theta_{\text{PtO}}, \theta_{\text{PtO}} = a_3 + b_3 \cdot E$		
$E/V$	1.0–1.15	1.25–1.5
$a_2$	−9.99	−13.8
$b_2/V^{-1}$	10.8	13.9
$a_3$	−1.95	−1.26
$b_3/V^{-1}$	2.19	1.57

$$\theta_{\text{PtO}} = a_3 + b_3 \cdot E, \quad (5)$$

where  $a_3$  and  $b_3$  are constants which are dependent on the potential range. The obtained values of  $a_2$ ,  $a_3$ ,  $b_2$ , and  $b_3$  are summarized in Table 1. Mathematically, a combination of Eqs. 3, 4, and 5 gives

$$\log i_M = (a_2 - 6.74 a_3) + (b_2 - 6.74 b_3)E. \quad (6)$$

Both the increase and decrease in  $i_M$  with increasing potential in Fig. 4 can be explained by using Eq. 6. The positive and negative values of  $(b_2 - 6.74 b_3)$  mean the increase and decrease in  $i_M$ , respectively. According to Table 1,  $(b_2 - 6.74 b_3)$  had  $-3.34$  and  $3.74 \text{ V}^{-1}$  in the potential ranges of 1.0–1.1 and 1.25–1.5 V, respectively. Although the change in  $b_3$  was only slight, the most significant factor of the change in the sign of  $(b_2 - 6.74 b_3)$  was  $b_3$ , i.e., the slope of the  $\theta_{\text{PtO}}$  vs.  $E$  plots.

**Slope of  $\theta_{\text{PtO}}$  vs.  $E$  Plots:** In the potential range 0.8–1.2 V, the slope of the  $\theta_{\text{PtO}}$  vs.  $E$  plots in the presence of methanol was slightly larger than that in its absence, as shown in Fig. 2. The change in the slope due to the presence of methanol was found to be due to a catalytic reduction of the oxygen layer with methanol, as follows.

Figure 7 shows the open-circuit decay after the oxygen layer is formed at several potentials in a methanol solution. As is known,<sup>10</sup> the arrest at about

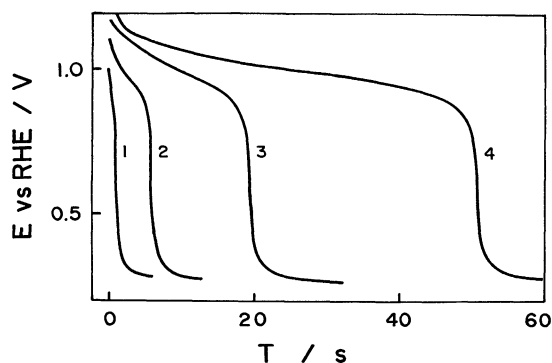


Fig. 7. Open circuit decays after preoxidation at several potentials in  $0.1 \text{ mol dm}^{-3} \text{ CH}_3\text{OH} + 0.5 \text{ mol dm}^{-3} \text{ H}_2\text{SO}_4$ . Preoxidation potentials (V): (1) 1.0; (2) 1.1; (3) 1.2; (4) 1.3.

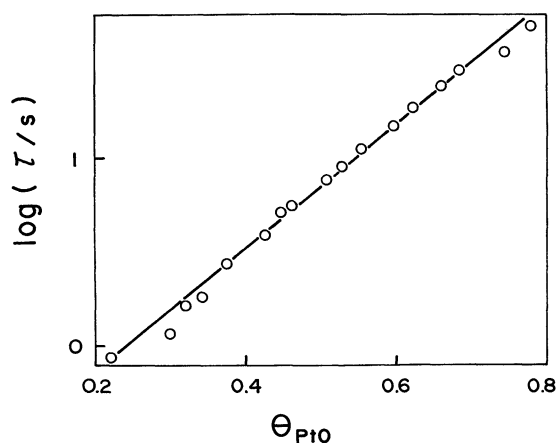


Fig. 8. Variation in transition time of open circuit decay with oxygen coverage,  $0.1 \text{ mol dm}^{-3} \text{ CH}_3\text{OH} + 0.5 \text{ mol dm}^{-3} \text{ H}_2\text{SO}_4$ .

1.2–0.8 V corresponds to a catalytic reduction of the oxygen layer with methanol. Expressing the transition time of the arrest at 1.2–0.8 V by  $\tau$ , a linear relationship between  $\theta_{\text{PtO}}$  and  $\log \tau$  was valid at coverages below about 0.8, as can be seen from Fig. 8.

$$\theta_{\text{PtO}} = a_1 + b_1 \log \tau, \quad (7)$$

where  $a_1$  and  $b_1$  are constants. Since the reduction rate,  $i_{\text{PtO}^{\text{red}}}$ , of the oxygen layer is  $2 \cdot Q_{\text{H}^0} \cdot (d\theta_{\text{PtO}}/dt)$ , the  $i_{\text{PtO}^{\text{red}}}$  can be expressed by

$$i_{\text{PtO}^{\text{red}}} = k_1 \cdot \exp(-m\theta_{\text{PtO}}), \quad (8)$$

where  $k_1$  and  $m$  are  $3.68$  and  $7.55 \times 10^{-4} \text{ A cm}^{-2}$ , respectively. According to Eq. 8, the  $i_{\text{PtO}^{\text{red}}}$  exponentially decreases with increasing  $\theta_{\text{PtO}}$ .

Also, in the case of the electrooxidation of methanol, a part of the oxygen layer will be reduced with methanol when the potential is sufficiently low. As

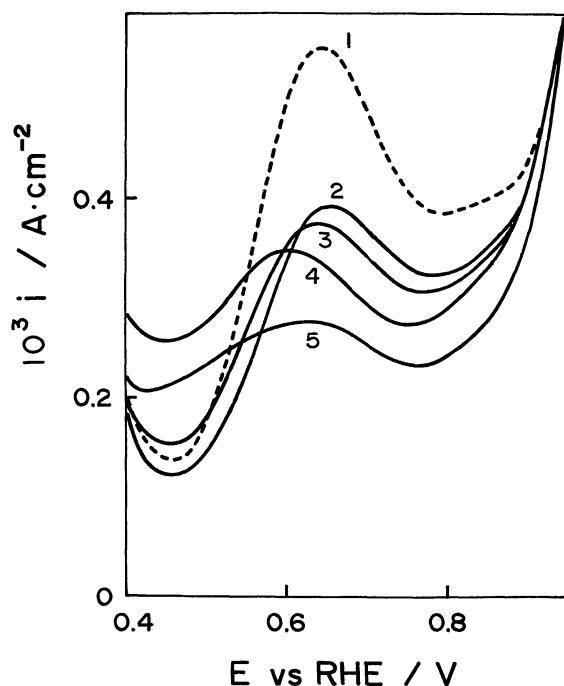


Fig. 9. Potentiodynamic  $i$ - $E$  curves immediately after preoxidation and subsequent reduction of oxygen layer,  $0.1 \text{ mol dm}^{-3} \text{ CH}_3\text{OH} + 0.5 \text{ mol dm}^{-3} \text{ H}_2\text{SO}_4$ , preoxidation time 10 s. Preoxidation potential (V): (1) without preoxidation; (2) 1.1; (3) 1.0; (4) 0.9; (5) 0.8.

shown in Fig. 2,  $\theta_{\text{PtO}}$  actually decreased in the presence of methanol at potentials below about 1.1 V, and  $b_3$  at such potentials was larger than that at higher potentials. The  $\theta_{\text{PtO}}$  also increased with increasing potential in the presence of methanol. According to Eq. 8, therefore, the  $i_{\text{PtO}^{\text{red}}}$  exponentially decreases with increasing potential. The large  $b_3$  in the low potential range is probably due to the potential dependence of  $i_{\text{PtO}^{\text{red}}}$ . From these results, it was concluded that the change in  $b_3$  in Table 1 was caused by a catalytic reduction of the oxygen layer with methanol.

**B) Retardation at 0.8–0.9 V:** For convenience, retardation due to the formation of an oxygen layer is hereafter called Retardation A. In the potential range of 0.8–0.9 V, some retardation due to another cause seems to occur, since the slopes of the  $\log i_{\text{M}}$  vs.  $\theta_{\text{PtO}}$  plots in Fig. 5 were extraordinarily small. The formation of new retarding substances other than the oxygen layer was confirmed by a potentiodynamic method (Fig. 1B). That is, the rate of the methanol oxidation was examined immediately after the preoxidation of methanol and then the reduction of the formed oxygen layer. Figure 9 shows the obtained  $i$ - $E$  curves for methanol oxidation. The solid and dotted curves in Fig. 9 indicate the  $i$ - $E$  curves with and without preoxidation, respectively. Hence, the smaller oxidation rate of the solid curve than that of the dotted curve indicates that some retardation other than Retardation

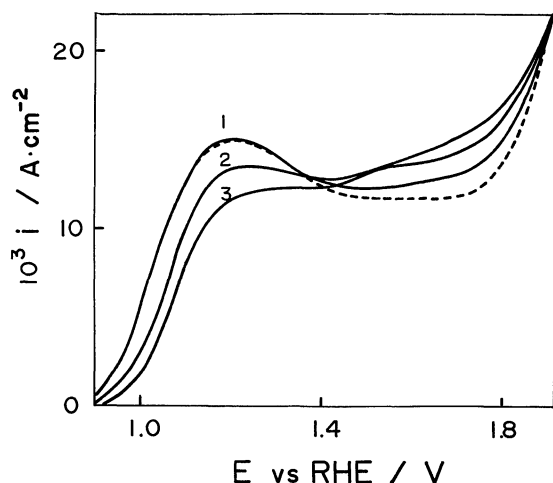


Fig. 10. Potentiodynamic  $i$ - $E$  curves for oxygen deposition immediately after preoxidation at 0.9 V in 0.1 mol dm<sup>-3</sup> CH<sub>3</sub>OH + 0.5 mol dm<sup>-3</sup> H<sub>2</sub>SO<sub>4</sub>, scan rate 20 V s<sup>-1</sup>, Preoxidation time (s): (1) 0.01; (2) 1.0; (3) 10. ----- in the absence of CH<sub>3</sub>OH.

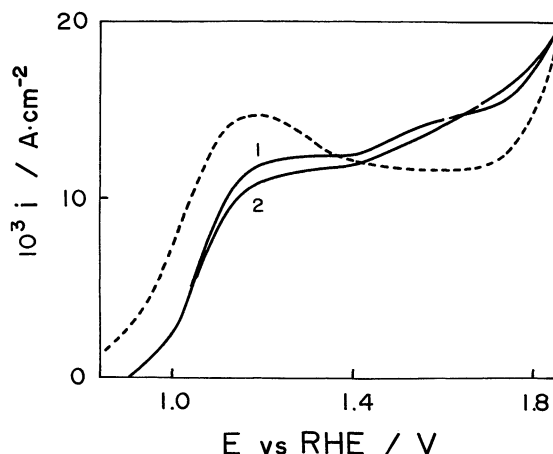


Fig. 11. Potentiodynamic  $i$ - $E$  curves for oxygen deposition immediately after preoxidation at 0.9 V, scan rate 20 V s<sup>-1</sup>, preoxidation time 10 s. Solutions: (1) 0.01 mol dm<sup>-3</sup> HCHO + 0.5 mol dm<sup>-3</sup> H<sub>2</sub>SO<sub>4</sub>, (2) 0.01 mol dm<sup>-3</sup> HCOOH + 0.5 mol dm<sup>-3</sup> H<sub>2</sub>SO<sub>4</sub>. ----- in the absence of HCHO and HCOOH.

A occurs. The retardation in Fig. 9 was most remarkable at a preoxidation potential of 0.8 V, and the extent of the retardation decreased with increasing preoxidation potential. Consequently, the discussion of Retardation A described in the preceding section was little influenced by the new retardation, since the dependence of the oxidation rate on the potential and oxygen coverage was only slight at high preoxidation potentials.

The formation of new retarding adsorbates could be confirmed by the oxygen-deposition method in Fig. 1A. At the scan rate of Fig. 10, the oxygen deposition was very fast in comparison with methanol oxidation. Consequently, the broad waves over the potential range of about 0.8–1.8 V in Fig. 10 virtually corresponded to the oxygen deposition, even in the presence of methanol. The solid lines in Fig. 10 indicate the  $i$ - $E$  curves for oxygen deposition after preoxidation of methanol at 0.9 V. This potential was convenient for the detection of a new adsorbate by the oxygen-deposition method, because both the oxidizable adsorbate, such as CO<sub>ad</sub>, and the predeposited oxygen were practically absent. The dotted line in Fig. 10 indicates the  $i$ - $E$  curve from 0.8 V in the supporting electrolyte alone, i.e., a curve without any predeposited oxygen and oxidizable adsorbate. From a comparison of the solid and dotted curves, the formation of nonreactive adsorbates from methanol was confirmed. Similar adsorbates have been reported in the case of the adsorption of some halogen ions<sup>11,12</sup> and acetic acid<sup>13</sup> on platinum electrodes, but have not so far been detected in the oxidation of methanol and related compounds. That is, the adsorbates which were detected in Fig. 10 were a new type in methanol oxidation. Judging from the magnitude of the

decrease in the rate of the oxygen deposition, the adsorbate amount increased with increasing time. Hence, the current decay, such as that in Fig. 3, can be explained in terms of the formation of this adsorbate.

As can be seen from Fig. 11, similar adsorbates were also detected in the presence of a small amount of formaldehyde and formic acid. In the case of formic acid, Kita et al.<sup>14</sup> attributed the retardation of its oxidation to the formation of a polymer-like adsorbate which was stabilized by hydrogen bonding at the oxygen atom. In the case of methanol oxidation, probably, the oxygen atom of the dehydrogenated methanol is stabilized by a similar bonding. In order to confirm the formation of the polymer-like adsorbate, however, further investigation is necessary.

**Mechanism of Methanol Oxidation in the Presence of Oxygen Layer.** The following equation can be derived from Eqs. 3 and 4.

$$i_M = k \exp(\alpha_n F E / RT) \cdot \exp(-m \theta_{PtO}), \quad (9)$$

where  $\alpha_n$  and  $m$  are constants. A similar equation has been proposed for oxygen deposition,<sup>15</sup> and explained in terms of charge transfer accompanied by an adsorption step. In the case of methanol oxidation, the adsorption of methanol molecules and some intermediates has been suggested.<sup>9,16,17</sup> The coverage dependence of  $i_M$  in Eq. 9 indicates a strong interaction between the adsorbed organic molecules and adsorbed oxygen. As is known,<sup>18</sup> the amount of adsorbates from methanol was too small to be detected by the usual method. This fact supports the idea that interacted adsorbates are the reactant, i.e., methanol molecules.

From these results, it was concluded that the rate-determining step in the presence of platinum oxide

was a methanol adsorption accompanied by some charge transfer.

#### References

- 1) V. S. Bagotzky and Yu. B. Vasylyev, *Electrochim. Acta*, **9**, 869 (1964); *ibid.*, **12**, 1323 (1967).
  - 2) S. Gilman, in "Electroanalytical Chemistry," ed by A. J. Bard, Marcel Dekker, New York (1967), Vol 2, p.142, 185.
  - 3) P. Delahay, in "Double Layer and Electrode Kinetics," Interscience (1965), p. 276.
  - 4) M. Hollnagel and U. Lohse, *Z. Phys. Chem.*, **232**, 237 (1966).
  - 5) R. A. Rightmire, R. L. Rowland, D. L. Boos, and D. L. Beals, *J. Electrochem. Soc.*, **111**, 242 (1964).
  - 6) S. N. Raicheva, S. V. Kalcheva, M. V. Christov, and E. I. Sokolova, *J. Electroanal. Chem.*, **55**, 213 (1974).
  - 7) T. Loucka and J. Weber, *J. Electroanal. Chem.*, **21**, 329 (1969).
  - 8) A. Capon and R. Parsons, *J. Electroanal. Chem.*, **44**, 239 (1973).
  - 9) H. Matsui, *Bull. Chem. Soc. Jpn.*, **61**, 3295 (1988).
  - 10) J. E. Oxley, G. K. Johnson, and B. T. Buzalski, *Electrochim. Acta*, **9**, 897 (1964).
  - 11) S. Gilman, *J. Phys. Chem.*, **68**, 2098 (1964); *ibid.*, **68**, 2112 (1964).
  - 12) V. S. Bagotzky, Yu. B. Vassilyev, J. Weber, and J. N. Pirtskhalava, *J. Electroanal. Chem.*, **27**, 31 (1970).
  - 13) A. Wiekowski, J. Sobkowski, P. Zelenay, and K. Franaszczuk, *Electrochim. Acta*, **26**, 1111 (1981).
  - 14) H. Kita and T. Katagiri, *Electroanal. Chem.*, **220**, 125 (1987).
  - 15) R. Woods, in "Electroanalytical Chemistry," ed by A. J. Bard, Marcel Dekker, New York (1976), Vol 9, p. 59.
  - 16) M. W. Breiter, *Discuss. Faraday Soc.*, **45**, 79 (1968).
  - 17) V. S. Bagotzky, Yu. B. Vassilyev, and O. A. Kazova, *J. Electroanal. Chem.*, **81**, 229 (1977).
  - 18) M. W. Breiter, in "Modern Aspects of Electrochemistry," ed by J. O'M. Bockris and B. E. Conway, Plenum Press, New York (1975), Vol 10, P. 205.
-